Distinct Effects of Homogeneous Weak Disorder and Dilute Strong Scatterers on Phase Competition in Manganites

Kalpataru Pradhan, Anamitra Mukherjee, and Pinaki Majumdar
Harish-Chandra Research Institute, Chhatnag Road, Jhusi, Allahabad 211 019, India
(Received 13 March 2007; published 3 October 2007)

We study the two orbital double-exchange model in two dimensions including antiferromagnetic (AFM) superexchange, Jahn-Teller coupling, and substitutional disorder. At hole doping $x = 0.5$ we focus on phase competition between the ferromagnetic metal (FMM) and the charge-ordered (CO) and orbital-ordered (OO) *CE* state and compare the impact of weak homogeneous disorder to that of a low density of strong scatterers. Even moderate homogeneous disorder suppresses the *CE*-CO-OO phase and leads to a glass with nanoscale correlations, while dilute strong scatterers of comparable strength convert the *CE*-CO-OO phase to a *phase separated* state with ferromagnetic metal and AFM-CO-OO clusters.

DOI: 10.1103/PhysRevLett.99.147206 PACS numbers: 75.47.Lx, 72.80.Ng, 75.47.Gk

The manganese oxides of the form $A_{1-x}A'_xMnO_3$ involve a remarkable interplay of charge, spin, lattice, and orbital degrees of freedom [1]. This cross coupling is most striking in the half doped ($x = 0.5$) manganites, many of which have a charge and orbital-ordered insulating (CO-OO-I) ground state with *CE* magnetic order—a zigzag pattern of ferromagnetic chains with antiferromagnetic (AFM) coupling between them. The *CE*-CO-OO-I phase shows up in manganites with low mean cation radius (r_A) while systems with large r_A are ferromagnetic metals (FMM). The variation of r_A leads to a ''bicritical'' phase diagram [2] with a first order boundary between the FMM and the *CE*-CO-OO-I phases.

Disorder has a remarkable effect on the bicriticality. Even moderate ''alloy'' disorder, due to random location of A and A' ions at the rare earth site, converts the CO-OO-*CE* phase to a short range correlated glass, but has only limited impact on the ferromagnet [2–4]. The asymmetric suppression of spatial order by cation disorder and the emergence of a charge-orbital-spin glass at low r_A are one set of intriguing issues in these materials. Unusually, while alloy type randomness on the A site leads to a *homogeneous glassy phase*, the substitution of a few percent of Mn (the B site) by Cr [5,6] leads to *phase separation* (PS) of the system [7–10] into FMM and AFM-CO-OO-I domains. The difference between A and B site disorder holds the key to the much discussed phase coexistence and spatial inhomogeneity in the manganites.

In this Letter we provide the first results on the relative effects of A and B type substitutional disorder on phase competition in a manganite model. We study weak ''alloy'' disorder and dilute strongly repulsive scatterers. Our main results are: (i) alloy disorder indeed leads to asymmetric suppression of long range order; moderate disorder converts long range *CE*-CO-OO to an *insulating glass* with nanoscale inhomogeneities, while FMM order is only weakened. (ii) A low density, $\gtrsim 4\%$, of strong scatterers in the *CE* phase leads to cluster coexistence of AFM-CO-OO and FMM regions and the ground state is a *poor metal*. (iii) The impact of strong scatterers depends crucially on whether they are attractive or repulsive, it correlates with the asymmetry of the ''clean'' system about $x = 0.5$, and uncovers a new route for phase control.

We consider a two band model for e_g electrons, Hund's coupled to t_{2g} derived core spins, in a two-dimensional square lattice. The electrons are also coupled to Jahn-Teller phonons, while the core spins have an AFM superexchange coupling between them. These ingredients are all necessary to obtain a *CE*-CO-OO phase. We include the effect of disorder through an on site potential.

$$H = \sum_{\langle ij\rangle\sigma}^{\alpha\beta} t_{\alpha\beta}^{ij} c_{i\alpha\sigma}^{\dagger} c_{j\beta\sigma} + \sum_i (\epsilon_i - \mu) n_i - J_H \sum_i \mathbf{S}_i \cdot \boldsymbol{\sigma}_i + J_{\mathrm{AFM}} \sum_{\langle ij\rangle} \mathbf{S}_i \cdot \mathbf{S}_j - \lambda \sum_i \mathbf{Q}_i \cdot \boldsymbol{\tau}_i + \frac{K}{2} \sum_i \mathbf{Q}_i^2. \quad (1)$$

Here, c and $c^{\dagger}$ are annihilation and creation operators for e_g electrons and α, β are the two Mne_g orbitals $d_{x^2-y^2}$ and $d_{3z^2-r^2}$, labeled (a) and (b) in what follows. $t_{\alpha\beta}^{ij}$ are hopping amplitudes between nearest-neighbor sites with the symmetry dictated form: $t_{aa}^{x} = t_{aa}^{y} \equiv t$, $t_{bb}^{x} = t_{bb}^{y} \equiv t/3$, $t_{ab}^{x} = t_{ba}^{x} \equiv -t/\sqrt{3}$, $t_{ab}^{y} = t_{ba}^{y} \equiv t/\sqrt{3}$, where x and y are spatial directions. We consider effectively a lattice of Mn ions and treat the alloy disorder due to cationic substitution as a random potential ϵ_i at the Mn site picked from the distribution $P_A(\epsilon_i) = \frac{1}{2}[\delta(\epsilon_i - \Delta) + \delta(\epsilon_i + \Delta)]$. The Cr doping case is modeled via $P_B(\epsilon_i) = \eta\delta(\epsilon_i - V) + (1 - \eta)\delta(\epsilon_i)$, where η is the percent substitution and V the effective potential at the impurity site. The e_g electron spin is $\sigma_i^{\mu} = \sum_{\sigma\sigma'}^{\alpha} c_{i\alpha\sigma}^{\dagger} \Gamma_{\sigma\sigma'}^{\mu} c_{i\alpha\sigma'}$, where the Γ's are Pauli matrices. It is coupled to the t_{2g} spin $\mathbf{S}_i$ via the Hund's coupling J_H, and we assume $J_H/t \gg 1$. λ is the coupling between the JT distortion $\mathbf{Q}_i = (Q_{ix}, Q_{iz})$ and the orbital pseudospin $\tau_i^{\mu} = \sum_{\sigma}^{\alpha\beta} c_{i\alpha\sigma}^{\dagger} \Gamma_{\alpha\beta}^{\mu} c_{i\beta\sigma}$, and K is the lattice stiffness. We set $t = 1$, $K = 1$, and treat the $\mathbf{Q}_i$ and $\mathbf{S}_i$ as classical variables [11]. The chemical potential μ is adjusted so that the electron density remains $n = 1/2$ which is also $x = 1 - n = 1/2$. For A type disorder the mean

 © 2007 The American Physical Society

value is $\bar{\epsilon}_i = 0$ and the variance is $\Delta_A^2 = \langle(\epsilon_i - \bar{\epsilon}_i)^2\rangle = \Delta^2$, while for B type disorder $\bar{\epsilon}_i = \eta V$ and $\Delta_B^2 = \langle(\epsilon_i - \bar{\epsilon}_i)^2\rangle = V^2\eta(1-\eta)$.

The clean CE ground state at $x = 0.5$ has been studied earlier [12–16] using mean field and Monte Carlo (MC) techniques and is well understood. The impact of disorder on the phase competition appropriate to $x = 0.5$ has been studied on small clusters [17–19] usually using simplified models either without orbital variables [18] or ignoring the electron-phonon coupling [19]. The difficulty of simulating the full model, Eq. (1), on a large system has prevented any conclusive study. We use our recently developed traveling cluster approximation (TCA) based MC [20] to solve the problem. Compared to exact diagonalization (ED) based MC which can handle typical sizes $\sim 8 \times 8$ we study the full model on lattices up to 40×40. In all our studies we use a moving cluster of size $\sim 8 \times 8$ [20] to anneal the spin and phonon variables.

Before discussing the effect of disorder we determine the clean ground state at $x = 0.5$ for varying $J_{\rm AFM}$ and λ, Fig. 1(a). At low λ and low $J_{\rm AFM}$ double exchange is the dominant interaction and kinetic energy optimization leads to a homogeneous ferromagnetic orbital-disordered charge-disordered (FM-OD-CD) state. This phase has a finite density of states at the Fermi level ϵ_F and is metallic. As $J_{\rm AFM}$ is increased, keeping the JT coupling small, a magnetic state emerges with peaks in the structure factor $S_{\rm mag}(\mathbf{q})$ at $\mathbf{q} = \{0, \pi\}$ or $\{\pi, 0\}$ (we call this the A-2D phase because of its similarity to the A-type phase in three dimensions), then an orbital ordered but uniform density CE phase, with simultaneous peaks at $\mathbf{q} = \{0, \pi\}, \{\pi, 0\}$, and $\{\pi/2, \pi/2\}$. At even larger $J_{\rm AFM}$ the dominant correlations are G type with a peak at $\mathbf{q} = \{\pi, \pi\}$. By contrast, increasing λ at weak $J_{\rm AFM}$ keeps the system ferromagnetic but leads to charge and orbital order (FM-CO-OO) for $\lambda \gtrsim 1.6$. Our interest is in a *charge-ordered CE* phase. Such a state shows up when both λ and $J_{\rm AFM}$ are moderately large. The TCA based phase diagram is broadly consistent with previous variational results [12,14–16] and with ED MC results on small systems [13]. Since the effect of disorder might be to create cluster coexistence [21,22] of phases *of different densities* that arise in the clean limit, Fig. 1(b) shows the phases and phase separation windows that occur at a typical coupling, $J_{\rm AFM} = 0.1$ and $\lambda = 1.6$. For these couplings the clean system is a CE-CO-OO phase at $x = 0.5$, a FMM for $x \lesssim 0.4$, and an A-2D type AFM for $x \gtrsim 0.55$.

In what follows we set $J_{\rm AFM} = 0.1$. This is in the right ballpark considering the AFM transition temperature at $x = 1$, and it allows close proximity of the CE and FMM phases. We mimic the bandwidth variation arising from changing r_A by varying λ/t across the boundary between CE-CO-OO and FM-OD-CD, and we now explore the effects of thermal fluctuation and disorder.

The key experiment [2] on the effect of A site disorder on bicriticality compared an "ordered" structure, where the rare earth and alkaline earth ions *sit on alternate layers*, with the "disordered" case where they are randomly distributed. The result is reproduced in the left panel in Fig. 2. While the ordered case has large transition temperatures for the CO-OO, CE, FM phases, etc., a random distribution of A and A' ions destroy the CO-OO-CE phase and partially suppresses the ferromagnetic T_c.

The right panel in Fig. 2 shows our result, where we superpose the clean phase diagram and the case with A type disorder $\Delta_A = 0.3$. In the clean limit at $T = 0$ as λ/t is increased there is a transition from a FMM to the A-2D phase at $\lambda/t \sim 1.52$, and then a transition to a CE-CO-OO phase at $\lambda/t \gtrsim 1.55$. On the FMM side, $\lambda/t \leq 1.52$, there is only a single thermal transition [23] at T_C as one cools the system. At large λ/t, however, cooling first leads to a CO-OO phase, at $T_{\rm CO}$, without magnetic order, followed by strong features in $S_{\rm mag}$ at $\mathbf{q} = \{0, \pi\}$ and $\{\pi, 0\}$, showing up at $T_{\rm SR}$, indicative of stripelike correlations. Finally, at a lower T the system makes a transition to CE order. If we set

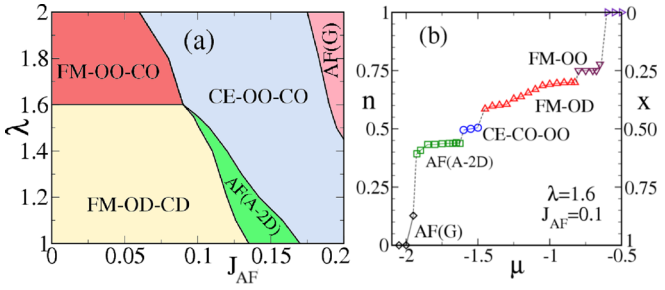

FIG. 1 (color online). (a) The ground state at $x = 0.5$ for varying $J_{\rm AFM}$ and λ, in the absence of disorder. (b) The doping ($n = 1 - x$) dependence of the ground state for varying chemical potential μ and typical electronic couplings, $\lambda = 1.6$ and $J_{\rm AFM} = 0.1$, near the FM-OD-CD and CE-CO-OO phase boundary. The phases in the vicinity of $x = 0.5$ are expected to show up in a cluster pattern on introducing disorder at $x = 0.5$.

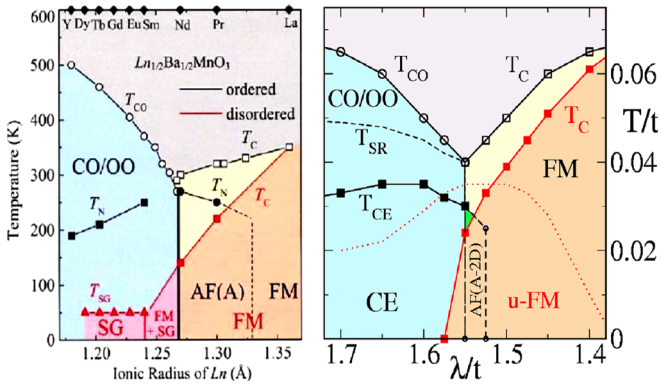

FIG. 2 (color online). (a) Experimental "bicritical" phase diagram in the $x = 0.5$ manganites obtained for ordered and disordered (alloy) structures. (b) Our results: superposed phase diagrams at $x = 0.5$ for $\Delta = 0$ and $\Delta = 0.3$. The long range CE-CO-OO for $\lambda > 1.55$ at $\Delta = 0$ is completely wiped out at $\Delta = 0.3$ while the FMM phase at low λ becomes an unsaturated FM with short range A-2D type correlations.

$t = 0.3$ eV, and use a factor of 3/2 to convert transition scales between 2D and 3D, our T_C at bicriticality would be ~200 K.

In the presence of A type disorder with $\Delta_A = 0.3$ we do not find any spatial order on the CE side in either the charge, orbital, or magnetic sector, down to $T \sim 0.005$. The absence of order in the CE-CO-OO side can be traced back to the "random field" ϵ_i coupling directly to the charge order parameter n_i. This breaks down charge correlations to the atomic scale. The ferromagnet being a $\mathbf{q} = 0$ state is more robust to A type disorder [18].

There are short range stripelike magnetic correlations that persist as peaks at $\mathbf{q} = \{0, \pi\}$ and $\{\pi, 0\}$ in $S_{\mathrm{mag}}(\mathbf{q})$. The onset of this feature is shown by the (red) dotted line in Fig. 2(b). This appears even on the ferromagnetic side below T_C. The T_C itself is somewhat suppressed by disorder and the ground state is an *unsaturated* ferromagnet (u-FM). Our analysis of the structure factor in the disordered system, however, does not suggest any coexistence of two distinct locally ordered phases at any λ. A type disorder in the bicritical regime does not induce phase coexistence. We have confirmed this directly from the spatial snapshots as well, as we discuss later. We have explored A type disorder with strength $\Delta_A = 0.1$, 0.2, 0.3, and 0.4, over the range of λ/t shown in Fig. 2(b). We now specialize to $\lambda/t = 1.6$, which is a CE-CO-OO phase near the clean phase boundary in Fig. 2(b), and we explore the impact of A type and B type disorder in detail. Figure 3(a) shows the T dependence of the major peaks in the spin, charge, and orbital structure factor in the clean limit at $\lambda/t = 1.6$, for reference, illustrating the distinct T_{CO}, T_{SR}, and T_{CE} scales.

The naïve expectation is that disorder would lead to cluster coexistence [21,22] of AFM-CO phases, that arise for $x \geq 0.5$, with the FMM phase at $x \lesssim 0.4$, Fig. 1(b). Figure 3(c) shows how the peaks in $S_{\mathrm{mag}}(\mathbf{q})$ evolve with Δ_A at low temperature ($T = 0.01$). The peak at $\mathbf{q} = \{\pi/2, \pi/2\}$ vanishes quickly, leading to a phase with stripelike correlations, and the $\mathbf{q} = \{0, \pi\}$, $\{\pi, 0\}$ peaks also vanish for $\Delta_A > 0.6$ leaving a glass. The response to B type disorder is more interesting. We have explored $V = 1$, 2, and 4 and $\eta = 2$, 4, and 8%. Since Cr is believed to be in a $t_{2g}^3 e_g^0$ state we focus here on $V = 2$ which is sufficiently repulsive to force $\langle n_i \rangle = 0$ (e_g^0 state) at the impurity sites. The response, as we vary the fraction of scatterers (η), is similar to A type at weak Δ_B. However, before the peak at $\mathbf{q} = \{0, \pi\}$, $\{\pi, 0\}$ vanishes we see the emergence of a peak at the ferromagnetic wave vector, $\mathbf{q} = \{0, 0\}$. There is a window at intermediate η where B type disorder leads to coexistence of FM and CO-OO-AFM regions. In terms of transport, Fig. 3(b), intermediate A type disorder strengthens the insulating character in $\rho(T)$, while B type disorder of comparable variance leads to an insulator-metal transition on cooling and a (poor) metallic state at low temperature.

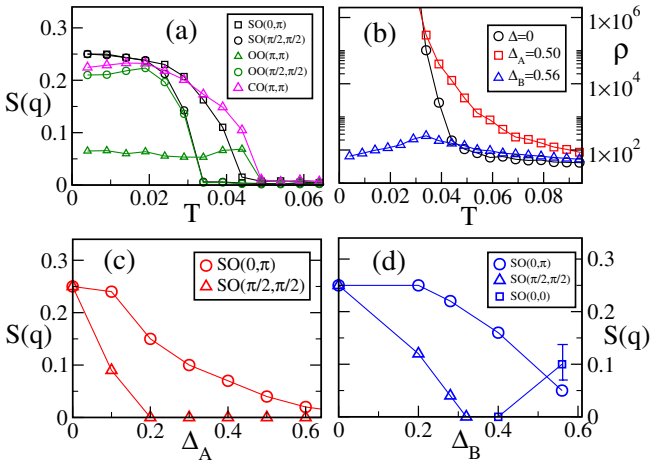

FIG. 3 (color online). Structure factors and resistivity $\rho(T)$ at $J_{\mathrm{AFM}} = 0.1$ and $\lambda/t = 1.6$. (a) The T dependence of the major peaks in the structure factor for spin order (SO), orbital order (OO), and charge order (CO) in the clean limit. Note the clear separation of scales between T_{CO}, T_{SR}, and T_{CE}. (b) $\rho(T)$ in the clean CE-CO-OO case and in the presence of A type and B type disorder, with $\Delta_A \approx \Delta_B \sim 0.5$. The Δ_B corresponds to $V = 2$ and dilution $\eta = 0.08$. (c) Variation of the major peaks in the magnetic structure factor with Δ_A at low temperature ($T = 0.005$). (d) Same as (c), now with B type disorder, $V = 2$ and varying η. Note the emergence of the FM $\mathbf{q} = \{0, 0\}$ peak around $\Delta_B = 0.4$ ($\eta = 0.04$).

The top row in Fig. 4 compares low temperature MC snapshots of the magnetic correlations in the clean system at $\lambda = 1.6$ (left) to that with $\Delta_A = 0.5$ (center) and $\Delta_B = 0.56$ (right). The respective panels in the middle row show the electron density $\langle n_i \rangle$ corresponding to the panels above. The panels at the bottom are the thermally averaged $S_{\mathrm{mag}}(\mathbf{q})$ in the three cases. In the clean limit the magnetic correlations are CE, with a checkerboard density distribution, and simultaneous magnetic peaks at $\mathbf{q} = \{0, \pi\}$, $\{\pi, 0\}$, and $\{\pi/2, \pi/2\}$. For A type disorder there are stripelike magnetic correlations with small (atomic scale) FM clusters but no signature of phase coexistence. The density field is also inhomogeneous in the nanoscale, with only short range charge correlations, and $S_{\mathrm{mag}}(\mathbf{q})$ has weak peaks at $\mathbf{q} = \{0, \pi\}$ and $\{\pi, 0\}$ but no noticeable feature at $\mathbf{q} = \{0, 0\}$. B type disorder, however, leads to FM *regions* coexisting with stripelike AFM correlations. The density field shows a corresponding variation, being roughly homogeneous within the FM droplets (with local density $n \sim 0.6$), and a CO pattern away from the FM regions. $S_{\mathrm{mag}}(\mathbf{q})$ now has peaks at $\mathbf{q} = \{0, \pi\}$, $\{\pi, 0\}$, *and* $\{0, 0\}$, as seen earlier in Fig. 3(d).

We explain the difference between the impact of A type and B type disorder as follows. (1) The introduction of A type disorder does not lead to coexistence of large FMM and AFM-CO-OO clusters, despite the presence of a PS window in the clean problem, Fig. 1(b), because (a) atomic scale potential fluctuations disallow CO coherence beyond

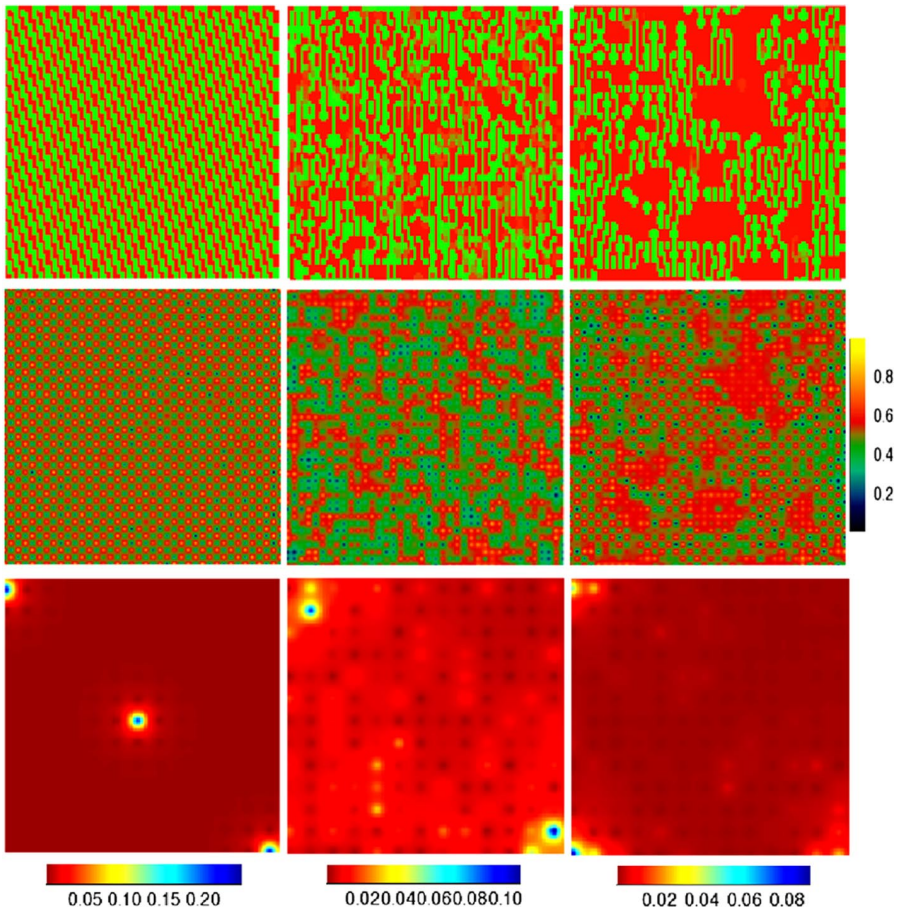

FIG. 4 (color online). MC snapshots and magnetic structure factor at low temperature, $T = 0.01$, size 40×40. Left row: $\lambda = 1.6$, nondisordered, middle row, $\lambda = 1.6$, A type disorder with $\Delta_{\text{eff}} = 0.5$, right row, $\lambda = 1.6$, B type disorder with $V = 2$, $\eta = 8\%$, $\Delta_{\text{eff}} = 0.56$. Top panel shows the nearest-neighbor magnetic correlation $\mathbf{S}_i \cdot \mathbf{S}_{i+\delta}$, where $\delta = x$ or y. Middle panel shows the charge density $\langle n_i \rangle$ for the configuration above. Bottom panels shows the MC averaged $S_{\text{mag}}(\mathbf{q})$. In each panel $\mathbf{q} = \{0, 0\}$ at the bottom left corner, $\mathbf{q} = \{\pi, 0\}$ at the bottom right corner, etc.

a few lattice spacings, while (b) homogeneous FMM clusters are destabilized by the disorder and become charge modulated. The result is a nanoscale correlated insulating glassy phase. (2) Dilute strongly repulsive scatterers act very differently: (a) they force an e_g^0 state at the impurity sites and generate an "excess density" 0.5η which has to be distributed among the remaining Mn sites, (b) the parent $x = 0.5$ CO phase cannot accommodate this excess charge homogeneously and the system prefers to phase separate into $x \sim 0.5$ AFM-CO and $x \sim 0.4$ FM clusters, (c) unlike the A type case, the FM clusters can survive and percolate since at low η there can be *large connected patches* without a B type site. We have verified this explicitly for several impurity configurations. Making the B site potential *strongly attractive* leads to a glassy AFM-CO state since carrier trapping reduces the effective electron count and forces the system towards a combination of $x \geq 0.5$ phases in Fig. 1(b).

In conclusion, we have reproduced all the key effects of A and B type disorder on phase competition in the half doped manganites. Our results suggest that B site impurities can be chosen to engineer phase control and the percolative conduction paths can be controlled through choice of dopant locations.

We acknowledge use of the Beowulf cluster at HRI and comments from E. Dagotto, S. Kumar, and P. Sanyal.

[1] See, e.g., *Colossal Magnetoresistive Oxides*, edited by Y. Tokura (Gordon and Breach, New York, 2000).
[2] D. Akahoshi *et al.*, Phys. Rev. Lett. **90**, 177203 (2003).
[3] R. Mathieu *et al.*, Phys. Rev. Lett. **93**, 227202 (2004).
[4] Y. Tokura, Rep. Prog. Phys. **69**, 797 (2006).
[5] A. Barnabe *et al.*, Appl. Phys. Lett. **71**, 3907 (1997).
[6] B. Raveau *et al.*, J. Solid State Chem. **130**, 162 (1997).
[7] T. Kimura *et al.*, Phys. Rev. Lett. **83**, 3940 (1999).
[8] T. Kimura *et al.*, Phys. Rev. B **62**, 15 021 (2000).
[9] H. Oshima *et al.*, Phys. Rev. B **63**, 094420 (2001).
[10] S. Mori *et al.*, Phys. Rev. B **67**, 012403 (2003).
[11] The validity of the classical approximations is studied in, e.g., E. Dagotto *et al.*, Phys. Rev. B **58**, 6414 (1998); A. C. M. Green, Phys. Rev. B **63**, 205110 (2001).
[12] J. van den Brink *et al.*, Phys. Rev. Lett. **83**, 5118 (1999).
[13] S. Yunoki *et al.*, Phys. Rev. Lett. **84**, 3714 (2000).
[14] L. Brey, Phys. Rev. B **71**, 174426 (2005).
[15] O. Cepas *et al.*, Phys. Rev. Lett. **94**, 247207 (2005).
[16] S. Dong *et al.*, Phys. Rev. B **73**, 104404 (2006).
[17] H. Aliaga *et al.*, Phys. Rev. B **68**, 104405 (2003).
[18] Y. Motome *et al.*, Phys. Rev. Lett. **91**, 167204 (2003).
[19] G. Alvarez *et al.*, Phys. Rev. B **73**, 224426 (2006).
[20] S. Kumar and P. Majumdar, Eur. Phys. J. B **50**, 571 (2006).
[21] Adriana Moreo *et al.*, Phys. Rev. Lett. **84**, 5568 (2000).
[22] S. Kumar and P. Majumdar, Phys. Rev. Lett. **92**, 126602 (2004).
[23] Our 2D magnetic "T_C" correspond to correlation length $\xi(T_C) \approx L$. There is no genuine T_C for $L \to \infty$ in 2D. The real 3D T_C will be $\approx 3/2$ times the 2D scale here.